doi.org/10.36721/PJPS.2025.38.6.REG.15175.1

Study on the analgesic mechanism of massage on NPP by LNCRNAH19 regulating miR-342-3p/IER3

Yingye Liang[1], Pingting Wu[2], Yuling Jiang[2], Dongming Lu[1], Peng Yang[3], Zhenbao Gan[1]* and Yufeng He[1]*

[1]The First Affiliated Hospital of Guangxi, University of Chinese Medicine, Nanning, Guangxi, China
[2]Guangxi University of Chinese Medicine, Nanning, Guangxi, China
[3]The Affiliated Fangchenggang Hospital of Guangxi University of Chinese Medicine, Fangchenggang, Guangxi, China

Abstract: Using a rat model of neuropathic pain, this study investigated the analgesic mechanism of massage therapy with an emphasis on the lncRNA H19/miR-342-3p/IER3 signaling pathway. Rats were split into control, model, sham, massage and lentiviral intervention groups using a spinal nerve ligation (SNL) paradigm. Molecular tests (qRT-PCR, Western blotting), behavioral evaluations (paw withdrawal thresholds and latencies) and ELISA were carried out. Massage reduced mechanical and thermal hyperalgesia by dramatically upregulating LncRNA H19 and IER3 expression and downregulating miR-342-3p and IL-17 levels. The effects of massage were replicated by intrathecal delivery of agolnc-H19a, thereby confirming H19's role in modulating the miR-342-3p/IER3 axis. By focusing on inflammatory signaling *via* the lncRNA H19/miR-342-3p/IER3 pathway, these results imply that massage alleviates neuropathic pain, providing new molecular understanding of the therapeutic benefits of massage.

Keywords: Analgesic mechanism; IER3; IL-17; LncRNA H19; Massage therapy; miR-342-3P; Neuropathic pain; Sciatic nerve ligation model

Submitted on 06-09-2025 – Revised on 20-09-2025 – Accepted on 11-10-2025

INTRODUCTION

According to the International Association for the Study of Pain, neuropathic pain results from somatosensory nerve system disorders or lesions (Li *et al*., 2020). Hyperalgesia, allodynia and spontaneous pain are some of its clinical manifestations. Systematic reviews place its global frequency between 6.9 and 10% (St. John Smith, 2018). According to (Wilkerson *et al*., 2020), the intricate pathophysiology of neurogenic pain syndromes makes current clinical management inadequate and emphasizes the need to better understand pain mechanisms in order to find novel therapeutic targets. Despite massage therapy's clinically validated analgesic effects, its underlying molecular pathways are still unknown, which restricts the possibility for therapeutic improvement. Traditional Chinese Medicine (TCM), which emphasizes meridian-centered mechanisms, offers an alternative paradigm for comprehending pain. "Qi-blood obstruction" is the cause of acute nociception, whereas "Qi-blood deficiency" is the cause of chronic discomfort (Yang *et al*., 2021). To address meridian imbalances, TCM massage uses specific, organized techniques like pushing, pressing and kneading. The foundation of the idea "restoring flow to relieve pain" is formed by these movements, which encourage Qi-blood circulation, clear obstacles and restore flow to reduce pain. Combining modern molecular techniques with TCM ideas provides an evidence-based viewpoint on therapeutic mechanisms. By highlighting prior research that connects TCM massage techniques to changes in physiological circuits related to pain, we offer justification for looking into the molecular mechanisms underlying massage analgesia.

According to (Lu *et al*., 2019), massage has been demonstrated to reduce neuropathic pain at the molecular level by upregulating immediate early response 3 (IER3), which is otherwise inhibited in NPP rat models. IER3 is controlled by the lncRNA H19/miR-342-3p axis, according to RNA sequencing research (Liu *et al*., 2019). We chose Long non-coding ribonucleic acid H19 (lncRNA H19), microRNA-342-3p (miR-342-3p) and IER3 in particular because previous research has shown that they play important roles in controlling neuronal excitability and inflammatory signaling; two processes that are essential in neuropathic pain. By examining this axis, we were able to link the effects of conventional massage therapy with quantifiable molecular results. Massage is thought to mediate analgesia by upregulating IER3, suppressing miR-342-3p activity, increasing lncRNA H19 expression and lowering the pro-inflammatory cytokine interleukin-17 (IL-17). By investigating the function of lncRNA H19 in the pathophysiology of neuropathic pain for the first time, this study improves pain management techniques and offers fresh perspectives on the molecular mechanisms underlying massage-based therapies.

MATERIALS AND METHODS

Animals

We got 42 healthy female Sprague-Dawley rats weighing

**Corresponding author:* e-mail: 19276723852@163.com; 510246833@qq.com

200-250g from Hunan Silaike Experimental Animal Company (License No. SCXK [Xiang] 2019-0004). The animals were kept in groups and subjected to the same conditions which included 12 hr light and dark cycles (08:00-20:00), a room temperature of 20-25°C and a relative humidity of 35-45%. Standard rodent chow and filtered water were provided ad libitum, with bedding materials and cages replaced daily to minimize environmental stressors.

Reagents and materials

agolnc-H19 lentiviral vectors and corresponding negative controls (GeneChem, Shanghai, China), tissue RNA preservation solution (Solarbio, Beijing, China), BCA protein quantification kit (Beyotime Biotechnology, Shanghai, China), Tris-HCl buffers (1.0 M, pH 6.8 and 1.5 M, pH 8.8; Solarbio), IL-17A ELISA kit (Elabscience, Wuhan, China) and 30% acrylamide solution (Solarbio). All chemical solutions were prepared using molecular biology-grade reagents.

Spinal nerve ligation (SNL) model

The experiment commenced following a 7-day acclimation period. Forty-two animals were randomly allocated into seven groups (n=6 per group) using a random number table: normal group, sham surgery group, model group, sham massage group, massage group, Lnc-H19a overexpression group (agolnc-H19a) and NC group. A neuropathic pain model was established through left L5 SNL, adapted from the protocol described by Kim and Chung (Lutolf *et al*., 2022). Under general anesthesia, the surgical site was prepared by shaving and disinfecting the skin approximately 3 cm lateral to the left posterior superior iliac spine. A 2 cm vertical incision parallel to the spinal column was made between the posterior superior iliac spine and vertebral column. After dissecting the deep fascia and musculature, two adjacent spinal nerves were identified and ligated with 5-0 absorbable chromic gut sutures. The wound was irrigated with sterile saline prior to layered closure using standard suturing techniques.

Model criteria

SNL model validation was based on gait alterations, mechanical withdrawal thresholds and thermal latency measurements. Successful induction was confirmed by observing spontaneous paw elevation, limb avoidance behaviors and abnormal gait patterns (e.g., dragging or hopping) in the affected hindlimb, accompanied by plantar flexion and eversion deformities. Quantitative validation required significant reductions in mechanical thresholds and thermal pain tolerance compared to baseline. Animals failing to meet these criteria were replenished through random selection. The model, massage and sham massage groups received standardized left L5 SNL ligation. Sham surgery controls underwent identical procedures with brief L5 spinal nerve exposure (2-3 minutes) without ligation. The normal group remained untreated throughout the study. For the agolnc-H19a and negative control (NC) groups, SNL modeling was performed following successful intrathecal catheterization.

Intrathecal catheterization

Intrathecal catheterization was performed under biological safety cabinet conditions following established protocols (Sakic, 2019; Lee & Chae, 2022). Following 12-hour fasting and 6-hour water deprivation, autoclaved surgical instruments and PE-10 catheters (alcohol-sterilized and thoroughly rinsed with saline) were prepared. Rats were anesthetized *via* intraperitoneal injection of 10% chloral hydrate until loss of hindpaw withdrawal reflex. Aseptic surgical technique included shaving and disinfecting the L6 vertebral region, followed by a 2-3 cm midline incision. Subcutaneous tissues were dissected to expose the L5-L6 intervertebral space. The PE-10 catheter was inserted at a 30-35° angle through the ligamentum flavum into the subdural space (3 cm advancement), with successful placement confirmed by tail flick response and saline flush patency. The catheter was secured *via* subcutaneous tunneling and sutured to the cervical musculature, leaving a 4 cm exteriorized segment heat-sealed at the terminus. Postoperative care included wound irrigation, layered closure and recovery in temperature-controlled individual housing with ad libitum water access for 12 hours.

Catheterization validation

Catheter functionality was verified three days post-operation through intrathecal injection of 10 µl of 2% lidocaine. Successful placement required immediate bilateral hindlimb paralysis with full motor recovery within 30 minutes. Animals demonstrating catheter-related complications (infection, catheter dislodgement, or obstruction) or failed pharmacological validation were excluded and replaced through randomized supplementation.

Massage therapy

Rats were securely restrained using fabric pouches and a specialized massage glove (PPS FingerTPS Tactile Measurement System, Shanghai Xingzhou Digital Technology Co., Ltd) was applied to stimulate the acupoints Huantiao (GB 30), Yanglingquan (GB 34) and Xuanzhong (GB 39) along the bilateral Gallbladder Meridian. The glove was set up to deliver a constant 4 N pressure before the studies began, guaranteeing reproducibility throughout sessions. A single, skilled researcher carried out each massage process using a predetermined order of pushing, pressing, kneading and plucking methods. To reduce unpredictability, every maneuver's sequence, length and pressure were carefully regulated. Each acupoint received one minute of stimulation per technique, totaling nine minutes per limb and 18 minutes per session (bilateral application). Treatments were administered daily for seven consecutive days. In order to account for handling and non-specific

tactile stimulation, rats in the sham massage group were given gentle, non-acupoint stroking of both hindlimbs for eighteen minutes every day for the same amount of time. In order to minimize sensory stimulation beyond general touch, care was taken to avoid applying direct pressure to acupoints. As a result, the sham intervention was able to isolate the unique effects of acupoint massage while matching the treated group in handling and duration. Normal, model and sham surgery groups were observed for seven days without intervention. The Lnc-H19a overexpression and negative control (NC) groups were established following the methodology of Hu *et al*. (Hu *et al*., 2023). On postoperative day 1, the overexpression group received an intrathecal injection of 10 μL agolnc-H19a lentivirus to upregulate Lnc-H19a expression, while the NC group received an equivalent dose of agolnc-H19a negative control lentivirus. Prior to injection, baseline thermal pain thresholds and gait alterations were assessed to confirm model validity. Mechanical and thermal pain thresholds were subsequently measured in both groups on days 3, 7, 10 and 14 post-injections. By ensuring consistency and closely resembling clinically applied acupoint therapy, this standardized, calibrated massage methodology increases the findings' translational significance.

Rationale for combining massage and intrathecal interventions

Following established aseptic protocols, intrathecal catheterization was used to precisely transport lentiviral constructs (agolnc-H19a or NC) to the spinal cord in order to mechanistically examine the analgesic effects of massage therapy. The lncRNA H19/miR-342-3p/IER3 signaling pathway was directly modulated by intrathecal treatments, whereas functional behavioral changes were assessed through massage therapy. By combining behavioral results with molecular investigations, this combination offers supplementary evidence that reinforces the causal relationships between the molecular pathways underpinning massage-induced analgesia.

Pain behavioral assessment in rats; Paw withdrawal mechanical threshold (PWMT, von frey test)

Mechanical pain thresholds were measured preoperatively (baseline) and on postoperative days 3 and 7. Rats were acclimated in a wire-mesh cage until spontaneous grooming and exploratory behaviors ceased. Von Frey filaments (4 g, 6 g, 8 g, 10 g, 15 g, 26 g, 60 g and 100 g) were sequentially applied to the plantar surface of the affected hind paw through the cage floor. A positive response (e.g., rapid paw withdrawal or licking) triggered by a filament defined the threshold. Each filament underwent 5-10 trials; a valid response threshold required 3-8 positive reactions within these trials. If no response occurred at 100 g, the threshold was recorded as 100 g. Three independent measurements, spaced 3 minutes apart, were averaged to determine the final threshold.

PWTL, Hargreaves test

Paw withdrawal thermal latency (PWTL) was measured preoperatively (baseline) and on postoperative days 3 and 7 using the Hargreaves method (Kumar *et al*., 2018). Rats were placed in an acrylic chamber mounted on a temperature-controlled platform preset to 52.5°C. Following acclimation (i.e., cessation of spontaneous grooming and exploratory behaviors), a timer was initiated. The latency to exhibit nociceptive behaviors (e.g., paw licking, withdrawal, or jumping) was recorded as the PWTL. To prevent tissue damage, the test was terminated at 30 seconds if no response occurred. Three measurements per rat were conducted at 5-minute intervals and the average value was calculated as the final PWTL.

Tissue and serum sampling

After administering pentobarbital sodium (50 mg/kg *via* intraperitoneal injection), the rats were euthanized *via* dislocation of the neck. Samples of blood were obtained through the abdominal aorta and were set to clot at room temperature for 30 minutes. The blood was then centrifuged at 3000 X g at 4 degrees Celsius for 15 minutes to separate the clot while the serum was obtained for further analysis. The serum was then stored at temperature -80 degrees Celsius and was set to be analyzed later.

For spinal tissue collection, the lumbar region was dissected to expose the spinal cord. Cut off the skin and muscle tissue to fully expose the L2-L6 segments of the spine. Use bone-biting forceps to clamp the L2 and L6 segments of the spine, respectively, while bending downwards with force to expose the spinal cord. Cut off the partially broken muscle tissue and spine with scissors, slowly pull out the spinal cord with force and then cut off the excess spinal cord, leaving only the L4-L6 segment. After placing it in a container, immediately put it under ice and then transfer it to a -80℃ freezer for storage.

ELISA analysis

Prior to the assay, reagent kits and serum samples were equilibrated to room temperature (18-25°C) for 30 min to minimize temperature-related variability. The wash buffer was prepared by diluting the concentrated solution with distilled water at a 1:24 ratio. For standard curve generation, lyophilized standards were reconstituted in 1 mL of assay diluent, vortexed gently for 1-2 min and centrifuged at 10,000 ×g for 1 min to remove particulates. Serial twofold dilutions were performed to generate concentrations ranging from 1,000 to 15.63 pg/mL, with 0 pg/mL as a blank control. Biotinylated detection antibodies and enzyme conjugates were prepared by centrifuging 100× stock solutions at 800 ×g for 1 min, followed by dilution to 1× working concentrations using the provided buffer. All solutions were degassed by brief centrifugation (800 ×g, 1 min) prior to use to eliminate air bubbles.

qRT-PCR analysis

The expression levels of LncRNA H19 and miR-342-3p in

rat spinal cord tissues were analyzed using quantitative real-time polymerase chain reaction (qPCR). Total RNA was extracted with TRIzol reagent and purified through sequential steps, including DEPC-treated water homogenization and chloroform phase separation. Reverse transcription was performed using the GoScript™ Reverse Transcription System (Promega) for LncRNA and the Mir-X™ miRNA First-Strand Synthesis Kit (Takara) for miRNA. For qPCR analysis, LncRNA H19 was amplified with GoTaq® qPCR Master Mix (Promega), while miR-342-3p was quantified using TB Green Premix Ex Taq™ (Takara). β-actin served as the endogenous control for normalization (Table 1).

Table 1: Primer sequences.

Gene	Primer sequence (5′ to 3′)
LncRNA H19-F	CTCCCAACAGAATGGCACATAG
LncRNA H19-R	CCATCTTGCCCTGTTTGACC
miR-342-3p	ACACAGAAATCGCACCCGTAA
β-actin-F	GGAGATTACTGCCCTGGCTCCTA

Note: Products were evaluated, and relative expression was calculated by formula (2−△△ct).

Western blot

The expression of IER3 in rat spinal cord tissues was analyzed *via* Western blotting. Protein samples were prepared by homogenizing tissues in lysis buffer, followed by quantification using a BCA protein assay kit. Proteins were separated by sodium dodecyl sulfate–polyacrylamide gel electrophoresis (SDS-PAGE) electrophoresis and transferred onto polyvinylidene fluoride (PVDF) membranes. Membranes were blocked with 5% non-fat milk, then incubated sequentially with primary and secondary antibodies. Target protein bands were visualized using chemiluminescent substrate and imaged with a gel documentation system. Densitometric analysis was performed using ImageJ software, with β-actin serving as the endogenous control for normalization.

Statistical analysis

As per statistical analysis done, which makes use of SPSS 20.0 statistical software, the results obtained are stated as a mean value ± the obtained standard deviation (SD). Prior to analysis, the dispersion of data was confirmed as normal. Differences in data obtained from two groups were evaluated by the use of independent samples t-tests, while data from more than two groups was assessed and analyzed through one-way ANOVA. For pairwise comparisons, the least significant difference (LSD) test was applied under the condition of variance homogeneity; otherwise, Tamhane's T2 test was applied. The value $P < 0.05$ was considered as being statistically significant.

RESULTS

Changes in the PWMT and PWTL

Repeated-measures ANOVA revealed significant interactions between groups and time points for both paw withdrawal mechanical thresholds (PWMTs, $F(16,112) = 5.369$, $P < 0.001$) and paw withdrawal thermal latencies (PWTLs, $F(16,112) = 17.279$, $P < 0.001$). No baseline differences were observed among groups prior to model induction ($P > 0.05$). Post-induction, the control group exhibited higher PWMT and PWTL values compared to all model-treated groups ($P < 0.05$). In the massage intervention group, PWMT and PWTL did not differ significantly from the model or sham massage groups at postoperative days 1 and 3. However, statistically distinct outcomes emerged by day 7 ($P < 0.05$), indicating delayed therapeutic efficacy of massage.

The control and sham surgery groups showed no significant temporal variations in PWMT or PWTL. In the model group, both thresholds decreased markedly at 1, 3, 7 and 14 days post-induction ($P < 0.05$), confirming successful model establishment. The sham massage group demonstrated a progressive decline in thresholds over time ($P < 0.05$), whereas the massage group exhibited a similar trend without reaching statistical significance ($P > 0.05$), suggesting partial mitigation of threshold reduction (Table 2; Figs. 1 and 2).

For mechanical nociception, no baseline differences existed between the agolnc-H19a and NC groups ($P > 0.05$). Although agolnc-H19a-treated rats showed numerically higher thresholds at days 3, 7 and 10 postoperatively, these differences were not statistically significant. By day 14, mechanical thresholds in the agolnc-H19a group (42.05 ± 4.76) significantly surpassed those in the NC group (28.16 ± 6.70, $P < 0.01$), paralleling the therapeutic effects of massage in restoring neuropathic pain thresholds (Table 3; Fig. 3).

Thermal nociception followed an analogous pattern: no baseline intergroup differences ($P > 0.05$), nonsignificant elevations in the agolnc-H19a group at early time points and a statistically robust increase by day 14 (agolnc-H19a: 23.24 ± 1.42 *vs.* NC: 16.97 ± 2.34, $P < 0.01$). These results indicate that intrathecal agolnc-H19a lentivirus administration mimics massage therapy in alleviating SNL-induced hyperalgesia and partially restoring thermal pain thresholds (Table 3; Fig. 4).

Comparative analysis of mRNA expression in rat spinal dorsal horn

On postoperative day 7, no significant difference in Lnc-H19 mRNA expression was observed between the naive and sham surgery groups ($P > 0.05$).

The model group exhibited reduced Lnc-H19 mRNA levels relative to the naïve group ($P < 0.05$), whereas the massage intervention group demonstrated a marked upregulation compared to both the model and sham massage groups ($P < 0.01$; Table 4, Fig. 5).

Table 2: PWMTs and PWTLs of the rats. The data are shown as X ± s (g, n=6).

	PWMT			PWTL		
Group	Before surgery	3 days after surgery	7 days after surgery	Before surgery	3 days after surgery	7 days after surgery
Control	113.16±13.82	113.33±14.00	113.55±14.17	49.83±6.12	47.90±3.46	48.88±3.76
Model	121.05±23.33	32.39±9.39*	13.11±4.05*	48.82±6.15	$11.67±1.59^{\#}$	$7.60±3.33^{\#}$
Sham-operated	112.94±13.64	70.33±11.31*	68.94±4.51	45.79±2.31	$22.83±4.35^{\#}$	22.61±7.14
Massage	108.33±15.46	$63.38±10.88*^{\triangle}$	$91.39±13.91^{\triangle}$	45.79±2.23	$22.49±2.61^{\#+}$	$43.42±6.96^{+}$
Sham massage	113.61±14.29	45.00±5.09*	57.16±10.40*	45.15±4.70	$18.82±4.06^{\#}$	$21.14±4.72^{\#}$

Note: ∗P < 0.05 compared with the control group; #P < 0.05 compared with the model group; ≥p < 0.05 vs. Sham massage group.

Table 3: Effects of intrathecal injection of agolnc-H19a lentivirus on mechanical and thermal pain thresholds in L5 SNL rats ($\bar{x}$ ±s,g,n=6).

	PWMT		PWTL	
Time	agolnc-H19a group	NC group	agolnc-H19a group	NC group
Baseline mechanical pain threshold (pre-surgery)	112.89±13.51	124.94±20.94	50.82±5.49	51.08±4.36
3 days after intrathecal injection	27.00±4.17	27.78±4.04	15.67±3.29	15.49±3.13
7 days after intrathecal injection	32.44±6.94	29.55±5.67	20.72±2.50	19.01±2.95
10 days after intrathecal injection	34.27±7.15	29.22±5.57	19.47±3.34	18.33±2.55
14 days after intrathecal injection	42.05±4.76*	28.16±6.70	$23.24±1.42^{\#}$	16.97±2.34

Note: Compared with the NC group, *P < 0.01. (NC: Negative control)

Table 4: Effects of manual therapy on mRNA expression in spinal cord tissue of L5 SNL rats ($\bar{x}$ ±s,$2^{-\triangle\triangle ct}$, n=6).

Group	Expression levels of LncRNA H19 mRNA	Expression levels of miR-342-3p
Control	1.00±0.00	1.00±0.00
Model	0.40±0.28*	$6.17±1.72^{\#}$
Sham-operated	1.18±1.03	3.00±2.91
Massage	6.40±1.70**	$0.63±0.51*^{\triangle}$
Sham massage	1.16±1.00	2.41±0.94

Note: *P < 0.05 *vs.* normal control group; **P < 0.01 *vs.* model group and △p < 0.05 *vs.* Sham massage group.

Table 5: Lnc-H19a and miR-342-3p expression profiles across treatment groups after intrathecal agolnc-H19a lentivirus delivery ($\bar{x}$ ±s,$2^{-\triangle\triangle ct}$,n=6).

Biomarker	agolnc-H19a group	NC group
Lnc-H19a	2.03±0.36*	1.00±0.00
miR-342-3p	0.35±0.13*	1.00±0.00

Note: *P < 0.01 *vs*. NC group.

Table 6: Differential IER3 expression in spinal cord of L5 SNL rats treated with manual therapy ($\bar{x}$ ±s, IER3/β-actin, n=6).

Group	IER3 protein expression levels	IL-17 expression levels
Control	1.00±0.00	22.72±1.99
Model	$0.27±0.13^{\#}$	$43.92±2.36^{\triangle}$
Sham-operated	0.97±0.20	37.97±1.18
Massage	$0.63±0.13^{\triangle}$	31.13±0.99*
Sham massage	0.32±0.09	34.70±1.76

Note: #P < 0.01 *vs.* normal control group; △P < 0.01 *vs.* model group and sham manual therapy group.

Table 7: Comparison of protein expression levels among experimental groups in rats following intrathecal injection of agolnc-H19a lentivirus ($\bar{x}$ ±s, IER3/β-actin, n=6) ($\bar{x}$ ±s, pg/mL, n=6).

Group	IER3 protein expression levels	IL-17 protein expression levels
agolnc-H19a group	1.45±0.24△	37.26±6.43#
NC group	1.00±0.00	65.83±7.03

Note: Compared with the NC group, △P < 0.01.

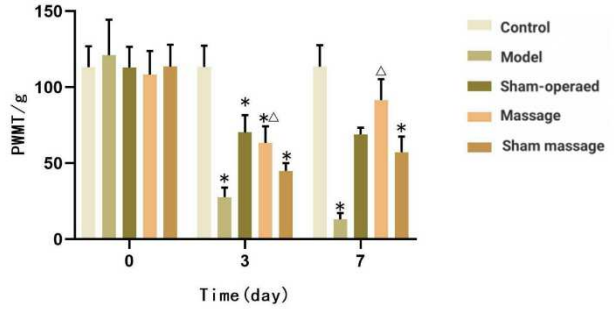

Fig. 1: Changes in PWMTs in rats following L5 spinal nerve ligation (SNL) at days 1, 3, and 7 days. *P < 0.05 *vs.* control; #P < 0.05 *vs.* model; ≥p < 0.05 *vs*. Sham massage group.

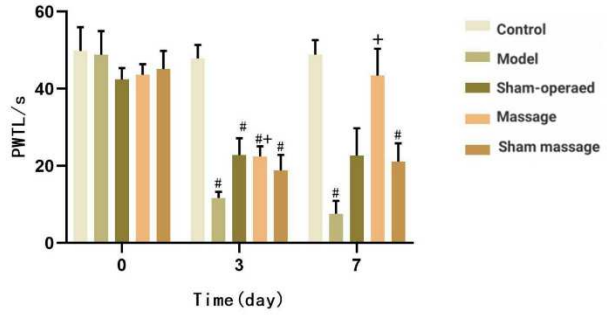

Fig. 2: Changes in PWTLs in rats following L5 SNL at days 1, 3 and 7. *P < 0.05 *vs.* control; #P < 0.05 *vs.* model.

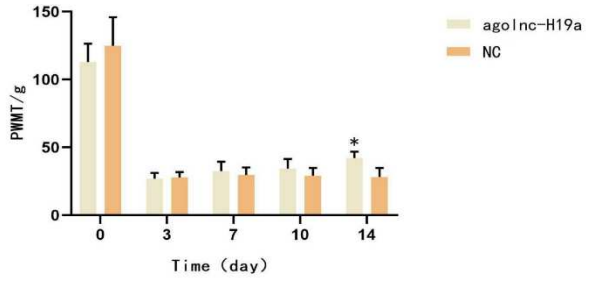

Fig. 3: Effects of massage and gene modulation on PWMT (von Frey test) following L5 SNL. Note: *P < 0.01 vs. NC group.

Similarly, miR-342-3p mRNA expression showed no baseline differences between the naïve and sham groups (P > 0.05). The model group displayed significantly elevated miR-342-3p levels compared to the naïve group (P < 0.01). In contrast, the massage group exhibited a substantial reduction in miR-342-3p expression relative to the model group (P < 0.01) and a statistically distinct profile compared to the sham massage group (P < 0.05; Table 4, Fig. 6).

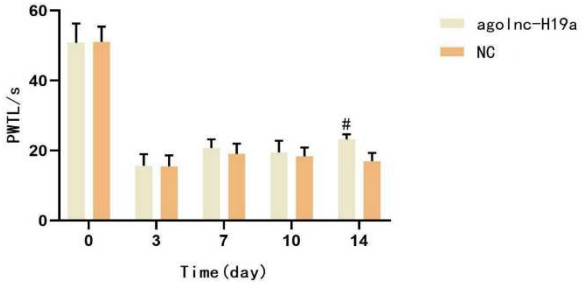

Fig. 4: Effects of massage and gene modulation on PWTL (Hargreaves test) following L5 SNL. Note: #P < 0.01 *vs.* NC group.

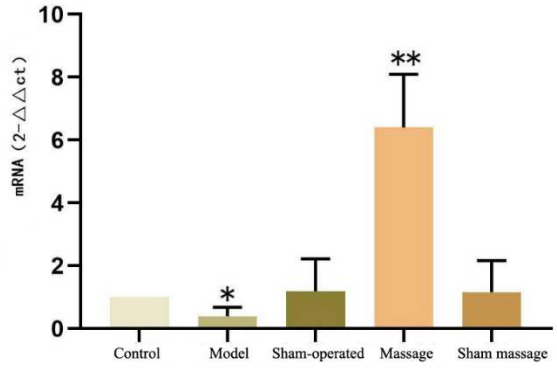

Fig. 5: Manual therapy modulates LncRNA H19 mRNA expression in the spinal cord of L5 (SNL) rats. Note: Data expressed as mean ± SD. *P < 0.05 *vs.* normal control; **P < 0.01 *vs.* model and sham groups.

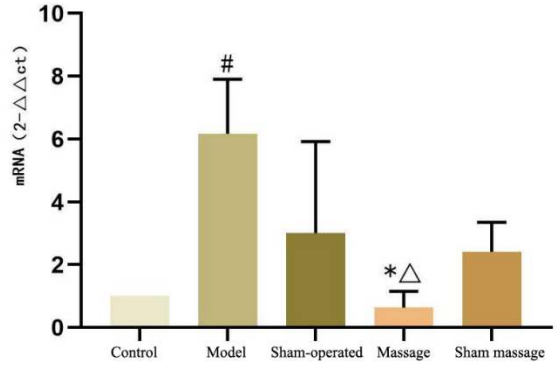

Fig. 6: Effects of manual therapy on LncRNA H19 mRNA expression in spinal cord tissue of L5 SNL rats. Note: *P <

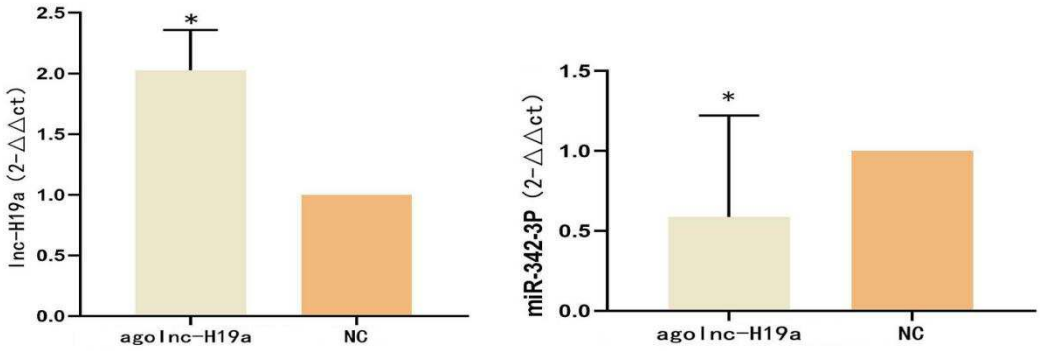

Fig. 7: Differential expression of LncRNA H19a and miR-342-3p in rats treated with agolnc-H19a lentivirus *via* intrathecal delivery.

0.05 *vs.* normal control group; **P < 0.01 *vs.* model group and △p < 0.05 *vs.* sham manual therapy group.

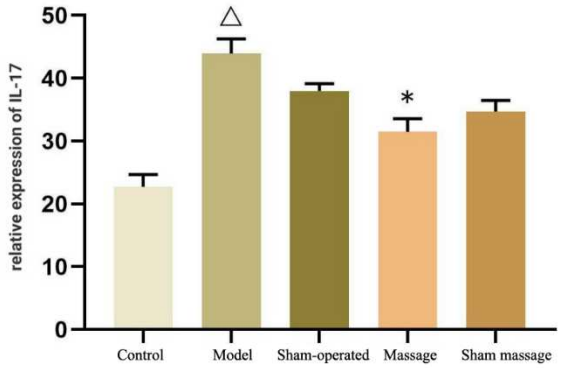

Fig. 8: Manual therapy attenuates serum IL-17 levels in neuropathic pain rats. Note: Data expressed as mean ± SD. △P < 0.01 *vs.* normal and sham surgery controls; *P < 0.01 *vs.* L5 SNL model and △p < 0.05 *vs.* sham manual therapy groups.

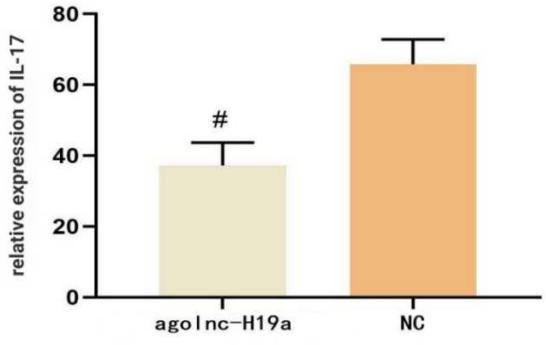

Fig. 9: Agolnc-H19a lentivirus modulates serum IL-17 expression in the spinal cord: A multi-group analysis. Note: Data expressed as mean ± SD. #P < 0.01 *vs.* NC group.

At 14 days post-intrathecal injection, agolnc-H19a-treated rats showed divergent expression patterns compared to the NC group (P < 0.01 for both targets). Lnc-H19a expression was elevated in the agolnc-H19a group, while miR-342-3p levels were suppressed, consistent with the therapeutic modulation observed in the massage intervention cohort (Table 5, Fig. 7).

Comparative analysis of protein expression in rat spinal dorsal horn

On postoperative day 7, IL-17 expression in the model group was significantly elevated compared to the naïve and sham surgery groups (P < 0.01). However, massage intervention markedly reduced IL-17 levels in the treatment group, with statistically distinct outcomes relative to both the model and sham massage cohorts (P < 0.01; Table 6, Fig. 8). At 14 days post-intrathecal injection, IL-17 expression differed significantly between the agolnc-H19a and NC groups (P < 0.01), with the agolnc-H19a group demonstrating suppressed IL-17 levels compared to NC controls (Table 7, Fig. 9). All IL-17 measurements reported in this study were performed using serum samples *via* ELISA.

For IER3 protein, no baseline differences were observed between the naïve and sham groups at day 7 (P > 0.05). The model group exhibited diminished IER3 expression relative to the naïve group (P < 0.01), whereas the massage group showed pronounced upregulation compared to both the model and sham massage groups (P < 0.01; Table 6, Fig. 10). Similarly, intrathecal agolnc-H19a administration resulted in divergent IER3 expression patterns by day 14 (P < 0.01 *vs*. NC group), with elevated IER3 levels in the agolnc-H19a cohort (Table 7, Fig. 11). These findings align with the therapeutic modulation observed in massage-treated rats, reinforcing the role of agolnc-H19a in mimicking manual intervention.

DISCUSSION

Theoretical basis and acupoint selection rationale for manual therapy

Although the traditional theoretical underpinning for massage treatment is provided by these TCM frameworks,

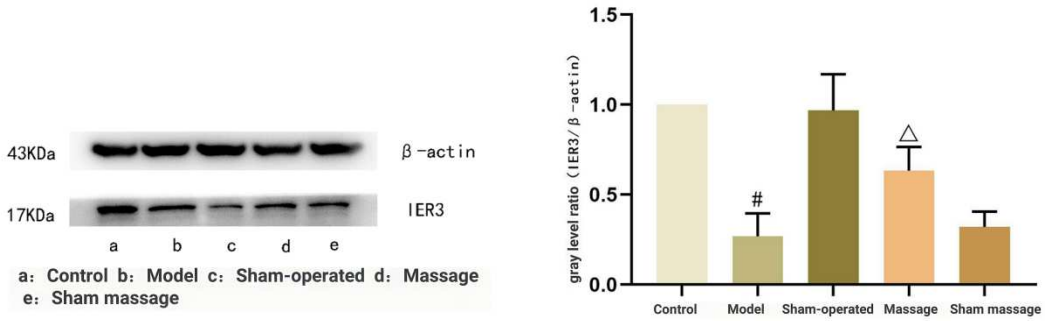

Fig. 10: Impact of massage therapy on ier3 protein expression in spinal cord tissue of L5 SNL model rats. Note: Data expressed as mean ± SD. △P < 0.01 *vs.* NC group.

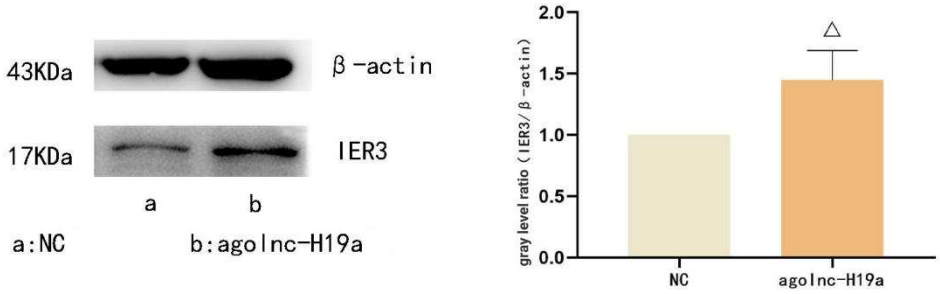

Fig. 11: agolnc-H19a lentivirus modulates IER3 protein expression in the spinal cord: A multi-group analysis.
Note: Data expressed as mean ± SD. △P < 0.01 *vs.* NC group.

the discussion's next sections mostly concentrate on molecular mechanisms that are backed by experimental data. The theoretical foundation of traditional Chinese manual therapy (Tuina) integrates meridian theory, qi-blood physiology, acupoint specificity, visceral organ theory, yin-yang and five-element principles and modern anatomical knowledge. According to meridian theory, meridians are channels for qi and blood circulation. These are confirmed by manipulating their corresponding channels and acupoints to regulate visceral function, relieve stagnation and regain physiological homeostasis (Wang *et al*., 2025). Qi-blood theory states that these substances underpin vital activities and their manual circulation helps relieve pain and dysfunction. Manual techniques promote the conditioning of these structures and promote their circulation which helps relieve pain and dysfunction. Acupoints specificity dictates targeted selection and intervention. Patently, distinct acupoints elicit specific therapeutic effects (e.g. analgesia, antiinflammation) on the selected pathology. Organ visceral theory emphasizes coordination among these organs, achieved indirectly through the regulation of meridians. The Yin-yang and Five element theory principles integrate all the above and provide guidance for therapeutic actions to restore imbalance among the opposites and their interelemental relations. Tuina gently aligns the findings of modern anatomy with the principles of traditional techniques. These principles nourish Tuina practice.

Neuropathic pain and the interplay of lncRNA H19, miR-342-3p and IER3 protein

This section, which is provided separately from the previously discussed TCM conceptual framework, focuses on the evidence-based biochemical mechanisms that underlie neuropathic pain and how massage can modulate them. Long non-coding RNAs (lncRNAs) as non protein-coding transcripts longer than 200 nucleotides, engage with gene expression at the structural and functional levels by means of epigenetics, regulation during the transcription phase and after transcription processes like miRNA sponging (Ransoho 2018). Newer researches emphasize their importance to NPP, with lncRNAs showing altered expression in the dorsal root ganglia (DRG) and spinal cord that drives nerve injury-associated neuronal hyperexcitability and pain sensitization (Li *et al* 2021). Among these is lncRNA H19, which is developmentally regulated, has lncRNA status and high expression during embryogenesis, but is turned off in the tissues of adults. H19 expression is upregulated in the non-neuronal cells of the DRG following peripheral nerve injury (Wen *et al*. 2020). This study seeks to understand the remaining H19

expression in the spinal dorsal horn and the temporal and spatial expression of H19 in the context of NPP, as well as its potential connection to pain modulation.

Small non-coding RNAs (≈14–24 nt) known as microRNAs (miRNAs) attach to 3′ untranslated regions to post-transcribe target genes (Juźwik *et al*., 2019; Karl *et al*., 2017; Liao *et al*., 2023). In the context of oncogenesis and inflammatory illnesses, MiR-342-3p, which is encoded within the EVL locus on chromosome 14q32, has been linked to apoptosis and inflammatory signaling (Jayawardana *et al*., 2016; Czimmerer *et al*., 2016; Song *et al*., 2019). Recent data indicates that miR-342-3p may interact with nociceptive signaling pathways and warrants additional investigation, despite the fact that its function in NPP is not entirely understood (Newton *et al*., 2024; Zhang *et al*., 2024; Dobosz *et al*., 2021; Kumar *et al*., 2020).

The gene IER3 (also known as IEX-1) is susceptible to stress and can affect the NF-κB and MAPK/ERK signaling pathways (Stindt *et al*., 2015; Wilcockson *et al*., 2023; Hong *et al*., 2018; Schneeweis *et al*., 2023). Neuropathy has been connected to the dysregulation of these pathways (Wei, 2018). The dynamic variations in IER3 expression in our initial SNL study suggested that it might regulate ERK activation linked to IL-17 in pain pathways.

Th17 cells and glial cells produce IL-17, a pro-inflammatory cytokine that accelerates neuroinflammation by triggering the NF-κB and MAPK pathways and raising the synthesis of TNF-α, IL-1β and IL-6 (Lee *et al*., 2018; Hu *et al*., 2023; Day *et al*., 2014; Simancas-Racines, 2018). IL-17's significance in peripheral and central sensitization is highlighted by the fact that IL-17 genetic deletion decreases pain behaviors and that DRG and spinal IL-17 overexpression is linked to mechanical allodynia in animal models (e.g., CCI) (Noma *et al*., 2011; Sun *et al*., 2017; Wang *et al*., 2022).

According to recent research, these molecules interact with one another. According to Liu *et al*. (2019), miR-342-3p can target and reduce IER3 and in other illness situations, LncRNA H19 has been demonstrated to block miR-342-3p. IER3 loss has been linked to increased IL-17 secretion (Rackov *et al*., 2022), indicating a regulatory network where IER3 → (modulates) IL-17 signaling and H19 → (inhibits) miR-342-3p → (derepresses). Our experimental results confirm this paradigm and provide credence to the idea that the H19/miR-342-3p/IER3 axis plays a role in massage-mediated analgesia. These results include H19 upregulation, decreased miR-342-3p, increased IER3 and decreased IL-17 after manual treatment.

Analysis of experimental findings

On postoperative day 3, SNL rats in the model group exhibited pronounced pain-related behaviors (e.g., limping, paw elevation and autotomy) alongside reduced mechanical and thermal pain thresholds. Manual therapy intervention improved these morphological and nociceptive parameters. By day 7, the massage group showed marked recovery in pain thresholds compared to the model group ($P < 0.01$), aligning with prior findings (Wang *et al*., 2024) that manual therapy's analgesic effects peak at 7 days post-injury before diminishing due to natural recovery. Notably, sham massage significantly lowered mechanical thresholds by day 3 ($P < 0.05$) but had no effect on thermal thresholds, suggesting mechanical nociception is more responsive to early intervention.

Following intrathecal injection of agolnc-H19a, both the agolnc-H19a and NC groups displayed reduced pain thresholds at day 3, confirming successful SNL modeling. While agolnc-H19a-treated rats showed gradual threshold improvements at days 7 and 10, statistical significance ($P < 0.01$) emerged only at day 14, indicating delayed therapeutic onset of the lentiviral construct.

Molecular analyses revealed that SNL injury suppressed L4–L6 spinal lncRNA H19 and IER3 expression while elevating miR-342-3p and IL-17 levels. Manual therapy reversed these trends, upregulating lncRNA H19 and IER3 while downregulating miR-342-3p and IL-17. Similar expression patterns were observed in agolnc-H19a-treated rats, suggesting shared regulatory mechanisms. Mechanistically, IL-17 released by Th17 cells activates spinal glia to amplify neuroinflammation and central sensitization. Downregulated IER3 exacerbates this process by disinhibiting IL-17 signaling, whereas miR-342-3p suppresses IER3 to promote inflammatory cascades. LncRNA H19 counteracts these effects *via* the miR-342-3p/IER3 axis, attenuating pro-inflammatory cytokine release. Although our study shows a strong relationship between massage therapy and the modulation of the H19/miR-342-3p/IER3 signaling axis, it should be highlighted that because no knockdown or inhibition experiments were conducted, clear molecular causality could not be shown. To improve the molecular knowledge of this system, future research using such focused manipulations is necessary. Collectively, manual therapy alleviates neuropathic pain by modulating this pathway to suppress spinal inflammation and nociceptive sensitization. Overall, these molecular insights support the theoretical viewpoints of TCM that were previously stated; nevertheless, our conclusions are supported by experimental data. In order to expand translational interpretation, the TCM elements are merely provided as conceptual parallels. Although our study shows a strong relationship between massage therapy and the modulation of the H19/miR-342-3p/IER3 signaling axis, it should be highlighted that because no knockdown or inhibition experiments were conducted, clear molecular causality could not be shown. To improve the molecular knowledge of this system, future research using such focused manipulations is necessary.

Limitations

We acknowledge that our findings have a number of limitations that should be taken into account. First, the sample size was modest (n = 6 each group), which could restrict the conclusions' generalizability and statistical power. Second, the study did not test the long-term effects or potential delayed effects of massage therapy on neuropathic pain; instead, it solely evaluated short-term outcomes. Third, just one animal model was employed, which was the rat SNL paradigm. Although widely acknowledged, it falls short of accurately simulating the complexity and diversity of neuropathic pain pathways found in humans. Fourth, while associations between massage therapy and the H19/miR-342-3p/IER3 axis were noted, there was no direct mechanistic proof (such as knockdown or inhibition trials) to support these findings. Lastly, there is a chance that the simulated massage control will still have tiny sensory effects, which could somewhat cloud the assessment of the precise effectiveness of acupoint-directed massage.

CONCLUSION

Manual therapy intervention significantly alleviated mechanical and thermal hyperalgesia in SNL rats by elevating their pain thresholds. Mechanistically, this analgesic effect may involve multi-level regulation of molecular mediators: upregulation of lncRNA H19 and IER3 expression, concurrent suppression of miR-342-3p and subsequent reduction in pro-inflammatory cytokine IL-17 levels. These coordinated changes suggest that manual therapy mitigates neuropathic pain by modulating the lncRNA H19/miR-342-3p/IER3 axis, thereby attenuating spinal neuroinflammation and nociceptive sensitization.

Acknowledgements

This work was supported by the National Natural Science Foundation of China (grant nos. 82160943, 82205305 and 82405603) and the Natural Science Foundation of Guangxi Province (grant nos. 2024GXNSFAA010377 and 2023GXNSFDA026012).

Author's contributions

Yingye Liang and Pingting Wu contributed equally to this work. Yingye Liang and Pingting Wu performed the experimental studies, data collection and initial data analysis. Yuling Jiang and Dongming Lu assisted with methodology development and laboratory supervision. Peng Yang contributed to data interpretation and critical revision of the manuscript. Zhenbao Gan and Yufeng He conceived and designed the study, supervised the research process, and finalized the manuscript. All authors read and approved the final version of the manuscript.

Funding

This research was supported by the National Natural Science Foundation of China (Grant Nos. 82160943, 82205305, and 82405603) and the Natural Science Foundation of Guangxi Province (Grant Nos. 2024GXNSFAA010377 and 2023GXNSFDA026012).

Data availability statement

The datasets generated and/or analyzed during the current study are available from the corresponding author on reasonable request.

Ethical approval

This study was reviewed and approved by the Institutional Animal Care and Use Committee (IACUC) of Guangxi University of Chinese Medicine under the ethical approval number DW20230302-017.

Conflict of interest

The authors declare that they have no conflict of interest regarding the publication of this paper.

REFERENCES

Czimmerer Z, Varga T, Kiss M, Daniel B, Ruzsicska B, Komuves L, Nagy G and Nagy L (2016). The IL-4/STAT6 signaling axis establishes a conserved microRNA signature in human and mouse macrophages regulating cell survival via miR-342-3p. *Genome Med.*, **8**(1): 63.

Day YJ, Liou JT, Lee CM, Chou AH, Liu FC, Mao CC and Shen YC (2014). Lack of interleukin-17 leads to a modulated microenvironment and amelioration of mechanical hypersensitivity after peripheral nerve injury in mice. *Pain.*, **155**(7): 1293–1302.

Dobosz E, Wadowska M, Kaminska M, Wilamowski M, Honarpisheh M, Bryzek D and Koziel J (2021). MCPIP-1 restricts inflammation via promoting apoptosis of neutrophils. *Front. Immunol.*, **12**: 627922.

Hong SK, Wu PK and Park JI (2018). A cellular threshold for active ERK1/2 levels determines Raf/MEK/ERK-mediated growth arrest versus death responses. *Cell Signal.*, **42**: 11–20.

Hu QQ, He XF, Ma YQ, Ma LQ, Qu SY, Wang HZ, Zhao Y and Jiang YL (2023). Dorsal root ganglia P2X4 and P2X7 receptors contribute to diabetes-induced hyperalgesia and the downregulation of electroacupuncture on P2X4 and P2X7. *Purinergic Signal.*, **19**(1): 29–41.

Hu X, Xu W, Ren Y, Wang Z, He X, Huang R, Huang J, Xu L and Cheng L (2023). Spinal cord injury: Molecular mechanisms and therapeutic interventions. *Signal Transduct. Target Ther.*, **8**(1): 245.

Jayawardana K, Schramm SJ, Tembe V, Thompson JF, Scolyer RA and Mann GJ (2016). Identification, review and systematic cross-validation of microRNA prognostic signatures in metastatic melanoma. *J. Invest. Dermatol.*, **136**(1): 245–254.

Juzwik CA, Drake SS, Zhang Y, Paradis-Isler N, Sylvester A, Amar-Zifkin A, Krichevsky AM and Fournier AE

(2019). MicroRNA dysregulation in neurodegenerative diseases: A systematic review. *Prog. Neurobiol.*, **182**: 101664.

Karl F, Griesshammer A, Uceyler N, Sommer C and Mey L (2017). Differential impact of miR-21 on pain and associated affective and cognitive behavior after spared nerve injury in B7-H1 knockout mouse. *Front. Mol. Neurosci.*, **10**: 219.

Kumar A, Kaur H and Singh A (2018). Neuropathic pain models are caused by damage to the central or peripheral nervous system. *Pharmacol. Rep.*, **70**(2): 206–216.

Kumar S, Fairmichael C, Longley DB and Turkington RC (2020). The multiple roles of the IAP superfamily in cancer. *Pharmacol. Ther.*, **214**: 107610.

Lee GA, Lin TN, Chen CY, Mau SY, Huang WZ, Kao YC, Liao NS and Liou CW (2018). Interleukin-15 blockade protects the brain from cerebral ischemia-reperfusion injury. *Brain Behav. Immun.*, **73**: 562–570.

Lee IS and Chae Y (2022). Exploring acupuncture actions in the body and brain. *Innov. Acupunct. Med.*, **15**(3): 157–162.

Liao J, Chen B, Zhu Z, Du C, Gao S, Zhao G, Huang W and Zhang Y (2023). Long noncoding RNA H19: An essential developmental regulator with expanding roles in cancer, stem cell differentiation and metabolic diseases. *Genes Dis.*, **10**(4): 1351–1366.

Li Z, Li X, Jian W, Xue Q and Liu Z (2021). Roles of long non-coding RNAs in the development of chronic pain. *Front. Mol. Neurosci.*, **14**: 760964.

Li X, Yuan J and Qin BY (2020). Research progress on PKC in the mechanism of neuropathic pain. *Med. Recapitul.*, **26**(10): 1924–1929.

Liu Z, Liu L, Zhong Y, Cai M, Gao J, Tan C, Han X, Guo R and Han L (2019). LncRNA H19 overexpression inhibited Th17 cell differentiation to relieve endometriosis through the miR-342-3p/IER3 pathway. *Cell Biosci.*, **9**(1): 84.

Lu DM, Tang HL, Wang KL, Liu FY, Liang ZJ and Huang R (2019). Clinical observation on the treatment of cervical spondylotic radiculopathy based on Shujing theory. *Lishizhen Med. Mater. Med. Res.*, **30**(3): 625–627.

Lutolf R, De Schoenmacker I, Rosner J, Sirucek L, Schweinhardt P, Curt A and Hubli M (2022). Anti- and pro-nociceptive mechanisms in neuropathic pain after human spinal cord injury. *Eur. J. Pain.*, **26**(10): 2176–2187.

Newton K, Strasser A, Kayagaki N and Dixit VM (2024). Cell death. *Cell.*, **187**(2): 235–256.

Noma N, Khan J, Chen IF, Matsuo A, Yoshizawa M and Sato T (2011). Interleukin-17 levels in rat models of nerve damage and neuropathic pain. *Neurosci. Lett.*, **493**(3): 86–91.

Ransohoff JD, Wei Y and Khavari PA (2018). The functions and unique features of long intergenic non-coding RNA. *Nat. Rev. Mol. Cell Biol.*, **19**(3): 143–157.

Sakic B (2019). Cerebrospinal fluid collection in laboratory mice: Literature review and modified cisternal puncture method. *J. Neurosci. Methods.*, **311**: 402–407.

Schneeweis C, Diersch S, Hassan Z, Krauss L, Schneider C, Lucarelli D, Rudalska R and Schneider G (2023). AP1/Fra1 confers resistance to MAPK cascade inhibition in pancreatic cancer. *Cell Mol. Life Sci.*, **80**(1): 12.

Simancas-Racines D (2018). Interventions for treating acute high-altitude illness. *Cochrane Database Syst. Rev.*, **2018**(6): CD009567.

Song X, Jin Y, Yan M, Chen H, Liu Q and Li X (2019). MicroRNA-342-3p functions as a tumor suppressor by targeting LIM and SH3 protein 1 in oral squamous cell carcinoma. *Oncol. Lett.*, **17**(1): 688–696.

St John Smith E (2018). Advances in understanding nociception and neuropathic pain. *J. Neurol.*, **265**(2): 231–238.

Stindt MH, Muller PA, Ludwig RL, Kehrloesser S, Dotsch V and Vousden KH (2015). Functional interplay between MDM2, p63/p73 and mutant p53. *Oncogene.*, **34**(33): 4300–4310.

Sun C, Zhang J, Chen L, Gao Y, Xu Y and Xu Y (2017). IL-17 contributed to the neuropathic pain following peripheral nerve injury by promoting astrocyte proliferation and secretion of pro-inflammatory cytokines. *Mol. Med. Rep.*, **15**(1): 89–96.

Wang Q, Shen Y, Lu J, Chen Y and Jin Y (2025). The academic thought of "reinforcing healthy Qi and unblocking regulation" in JIN Yicheng's Shanghai-style pediatric Tuina school and its clinical application. *J. Acupunct. Tuina Sci.*, pp.1–10.

Wang SH, Ma F, Tang ZH, Zhang Y, Luo P and Han J (2022). Correction to: Long non-coding RNA H19 regulates FOXM1 expression by competitively binding endogenous miR-342-3p in gallbladder cancer. *J. Exp. Clin. Cancer Res.*, **41**(1): 55.

Wang TY, Tang HL, Liang YY, Zhang FY and Li Y (2024). Effects of Zhuang medicine meridian-sinew Tuina on BRCC3-mediated NLRP3 deubiquitination and analgesic mechanisms in rats with neuropathic pain. *Mod. J. Integr. Tradit. Chin. West Med.*, **33**(1): 17–21.

Wei BL (2018). Effect and mechanism of Tuina on chronic neuropathic pain in rats based on the ERK signaling pathway. Doctoral dissertation, Guangxi Medical University.

Wen J, Yang Y, Wu S, Zhang H, Liu L and Hu X (2020). Long noncoding RNA H19 in the injured dorsal root ganglion contributes to peripheral nerve injury-induced pain hypersensitivity. *Mol. Pain.*, **7**(2): 176–184.

Wilcockson SG, Guglielmi L, Rodriguez PA, Amoyel M and Hill CS (2023). An improved Erk biosensor detects oscillatory Erk dynamics driven by mitotic erasure during early development. *Dev. Cell.*, **58**(23): 2802–2818.

Wilkerson JL, Jiang J, Felix JS, Bray JK, da Silva L, Gharaibeh RZ, Hunter KW and Schmittgen TD (2020).

Alterations in mouse spinal cord and sciatic nerve microRNAs after the chronic constriction injury (CCI) model of neuropathic pain. *Neurosci. Lett.*, **731**: 135029.

Yang P, Lu DM, Tang HL, Li JH and Chen J (2021). Clinical observation of Shujing Tuina therapy in treating acute lumbar sprain. *Liaoning J. Tradit. Chin. Med.*, **48**(1): 162–164.

Zhang C, Liu H, Peng Y, Ding W and Cao J (2024). Intelligent prediction and application research on soft rock tunnel deformation based on the ICPO-LSTM model. *Buildings*, **14**(7): 2244.